

# Consistent off-shell $\pi NN$ vertex and nucleon self-energy

S. Kondratyuk and O. Scholten

*Kernfysisch Versneller Instituut, 9747 AA Groningen, The Netherlands*

(Received 30 July 1998)

We present a consistent calculation of half-off-shell form factors in the pion-nucleon vertex and the nucleon self-energy. Numerical results are presented. Near the on-shell point the pion-nucleon vertex is dominated by the pseudovector coupling, while at large nucleon invariant masses we find a sizable pseudoscalar admixture. [S0556-2813(99)02002-6]

PACS number(s): 13.75.Gx, 14.20.Dh, 21.45.+v

## I. INTRODUCTION

The structure of hadronic vertices, usually parametrized in terms of form factors, is important in much of nuclear physics. The form factors may depend on the different invariants that can be constructed. In nucleon-meson or nucleon-photon vertices one often considers only the dependence on the momentum squared of the meson or photon. In the present paper we will consider so-called off-shell form factors where the dependence is studied on the momentum squared of one of the nucleons involved.

Off-shell form factors are an ingredient in the description of physical processes. For example, nucleon-photon off-shell form factors have been shown to be important in models for proton-proton bremsstrahlung [1–3] and virtual Compton scattering [4].  $\pi NN$  and other nucleon-meson form factors with an explicit dependence on the momentum of one or both nucleons have been used in models for  $NN$  [5] and  $\pi N$  [6–9] scattering, pion photoproduction [9] and vector meson production in nucleon-nucleon collisions [10]. In these models, the form factors have been phenomenologically parametrized, with the parameters adjusted to fit experimental data.

The off-shell structure of the nucleon-photon vertex [11–13], and the nucleon-pion vertex [11,14,15] has been studied before. In particular, dispersion relation techniques are used in Refs. [11,12,14], whereas the models of Refs. [13] are based on a perturbative dressing of the vertex with one-meson loops. In this work we investigate the pion-nucleon coupling in a field-theoretical model which is inherently non-perturbative and is based on the Schwinger-Dyson equation, considering loops to all orders. The nucleon self-energy and the pion-nucleon vertex function are both calculated in a consistent framework.

In general, off-shell form factors and the functions parametrizing the self-energy are complex functions, where the imaginary parts are related to open multiparticle channels of which the pion-nucleon channel will be the most important. Our approach is based on the analytic structure [16,11] of the nucleon self-energy and the off-shell  $\pi NN$  vertex, which is exploited by the use of dispersion relations. The imaginary parts of the form factors and the self-energy are calculated from Cutkosky rules [17]. To make this procedure tractable, we consistently neglect contributions to the imaginary parts from the multipion thresholds.

For the course of this paper, we are interested in vertices with one off-shell nucleon, which contain two independent form factors. The convergence of the loop corrections is in-

sured through the introduction of a “cutoff” function (the initial form factor). We obtained the interesting result that the widths of the converged form factors have an upper bound.

Solutions of the Schwinger-Dyson equation have been presented in the past (see, e.g., [18,19] and a recent paper [20]). There, a usually adopted approximation consists in assuming the same spin structure for the dressed and the bare vertex. The dressing of the vertex is thus parametrized in terms of a single form factor. In the present work we have released this condition and found a strong dependence of the spin structure of the vertex on the off-shellness involved.

Form factors are usually interpreted as representing the features that are not included explicitly in a particular model for a physical process, and as such, should be built consistently with the kind of models in which they are intended to be used. The form factors considered in the present paper are primarily designed for usage in a  $K$ -matrix model for pion-nucleon scattering, pion photoproduction, and Compton scattering off the nucleon [21,22]. Since in such a model the one-pion production channel is included explicitly, only the real form factor should be used there (at least below the two-pion threshold). This aspect is elaborated on in Sec. III C.

In any model, treatment of off-shell three-point vertices should be linked with treatment of higher-point vertices, because a redefinition of the nucleon field can change off-shell dependence of the former in favor of presence of the latter. The observables are oblivious to the representation of fields (this result is known as the equivalence theorem) [23], examples of which can be found, e.g., in Refs. [24–26]. In the present model, higher-point vertices are excluded at all stages of the calculations, and the discussion is carried out solely in terms of off-shell form factors in the  $\pi NN$  vertex.

The paper is organized as follows. In Sec. II the general structure of the off-shell  $\pi NN$  vertex is discussed. Our model is described in detail in Sec. III. At present we limit ourselves to the inclusion of one-pion-nucleon loops only, for which numerical results are presented in Sec. IV.

## II. STRUCTURE OF THE $\pi NN$ VERTEX

The  $\pi NN$  vertex operator is the sum of all connected Feynman diagrams with one incoming nucleon (carrying the momentum  $p$ ), one outgoing nucleon ( $p'$ ) and one pion ( $q = p - p'$ ), with the propagators for the external legs stripped away. The most general form compatible with Lorentz cova-

riance and isospin invariance reads [27]

$$\begin{aligned} \Gamma_\alpha(p', p, q) = & \tau_\alpha \left( \gamma^5 G_1(p'^2, p^2, q^2) + \gamma^5 \frac{\not{p} - m}{m} G_2(p'^2, p^2, q^2) \right. \\ & + \frac{\not{p}' - m}{m} \gamma^5 G_3(p'^2, p^2, q^2) \\ & \left. + \frac{\not{p}' - m}{m} \gamma^5 \frac{\not{p} - m}{m} G_4(p'^2, p^2, q^2) \right), \end{aligned} \quad (1)$$

where  $m$  denotes the nucleon mass and  $\tau_\alpha$ ,  $\alpha = 1, 2, 3$ , are the isospin Pauli matrices. The form factors  $G_i$  depend on the three Lorentz scalars,  $p'^2$ ,  $p^2$ , and  $q^2$ . Usually the situation is considered in which both nucleons are on the mass shell, i.e.,  $p'^2 = p^2 = m^2$ , and only  $G_1(m^2, m^2, q^2)$  enters in Eq. (1). In this paper we consider a different situation in which the pion and only one of the nucleons is on the respective mass shell,  $p'^2 = m^2$  and  $q^2 = \mu^2$ , where  $\mu$  denotes the pion mass. Such a vertex is conventionally called the half-off-shell  $\pi NN$  vertex, and it contains so-called half-off-shell form factors.

If the operator of Eq. (1) works on the positive energy spinor  $\bar{u}(p')$  to the left, the last two terms in Eq. (1) vanish due to the Dirac equation,  $\bar{u}(p')\not{p}' = \bar{u}(p')m$ , and the vertex contains only the form factors  $G_1(m^2, p^2, \mu^2)$  and  $G_2(m^2, p^2, \mu^2)$ . Similarly, if the initial nucleon is on-shell, only the form factors  $G_1(p'^2, m^2, \mu^2)$  and  $G_3(p'^2, m^2, \mu^2)$  are left. Charge-conjugation, space-inversion, and time-reversal symmetries allow us to relate these form factors:

$$\begin{aligned} G_1(p^2, m^2, \mu^2) &= G_1(m^2, p^2, \mu^2), \\ G_3(p^2, m^2, \mu^2) &= G_2(m^2, p^2, \mu^2). \end{aligned} \quad (2)$$

Hence, one can consider only the vertex with the outgoing on-shell nucleon. Omitting the trivial arguments in  $G_i$ ,

$$\begin{aligned} \Gamma_\alpha(m, p, \mu) &= \tau_\alpha \Gamma(m, p, \mu) \\ &= \tau_\alpha \gamma^5 \left( G_1(p^2) + \frac{\not{p} - m}{m} G_2(p^2) \right), \end{aligned} \quad (3)$$

where the notation  $\Gamma_\alpha(m, p, \mu)$  implies that  $q^2 = \mu^2$  and  $\bar{u}(p')\not{p}' = \bar{u}(p')m$  in all expressions for this vertex. Along with Eq. (3), we will use another form for the half-off-shell vertex,

$$\Gamma_\alpha(m, p, \mu) = \tau_\alpha \gamma^5 \left( G_{\text{PS}}(p^2) + \frac{\not{p} + m}{2m} G_{\text{PV}}(p^2) \right), \quad (4)$$

where

$$G_{\text{PS}}(p^2) = G_1(p^2) - 2G_2(p^2), \quad G_{\text{PV}}(p^2) = 2G_2(p^2), \quad (5)$$

denote the form factors corresponding to the usual pseudo-scalar and pseudovector couplings.

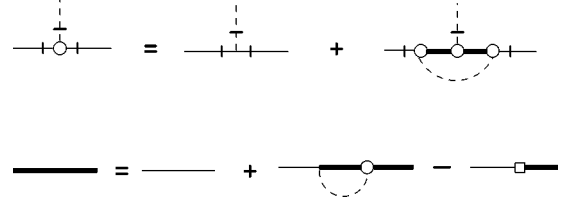


FIG. 1. The graphical representation of the system of Eqs. (6). The thin and thick solid lines correspond to the free and dressed propagators of the nucleon, respectively. The dashed line is the propagator of the pion. The circle indicates the dressed  $\pi NN$  vertex, and the square stands for the counterterm contribution to the nucleon self-energy. In the equation for the vertex the propagators of the external lines are stripped away, as indicated by the dashes on these lines.

### III. DESCRIPTION OF THE MODEL

The model for the form factors is based on a nonperturbative dressing of the vertex with pion loops as represented graphically in Fig. 1. The nucleon self-energy  $\Sigma(p)$  is calculated self-consistently using the Schwinger-Dyson equation [28] with the dressed vertex. This can be expressed in terms of a system of integral equations for the dressed  $\pi NN$  vertex  $\Gamma_\alpha(p', p, q)$  and the dressed nucleon propagator  $S(p)$ ,

$$\begin{aligned} \Gamma_\alpha(m, p, \mu) &= \Gamma_\alpha^0(m, p, \mu) - i \int \frac{d^4 k}{(2\pi)^4} [\Gamma_\beta(m, p' + k, k) \\ &\quad \times S(p' + k) \Gamma_\alpha(p' + k, p + k, \mu) S(p + k) \\ &\quad \times \Gamma_\beta(p + k, p, -k) D(k^2)], \\ S(p) &= S^0(p) + S(p) \Sigma(p) S^0(p), \end{aligned} \quad (6)$$

$$\begin{aligned} \Sigma(p) &= -i \int \frac{d^4 k}{(2\pi)^4} [\Gamma_\alpha(p, p + k, k) S(p + k) \\ &\quad \times \Gamma_\alpha^0(p + k, p, -k) D(k^2)] \\ &\quad - (Z_2 - 1)(\not{p} - m) - Z_2 \delta m, \end{aligned}$$

where  $D$  is the pion propagator,  $S^0$  is the free propagator of the nucleon, and  $\Gamma_\alpha^0(m, p, \mu)$  is the bare  $\pi NN$  vertex. The last two terms in the equation for the self-energy are part of the renormalization procedure and will be discussed later. The dressing is nonperturbative since the dressed vertex and propagator appear also on the right-hand side of the equations. As is well known, such a procedure suffers from divergences. In addition, we are interested to build a model for half-off-shell vertices while the right-hand sides of Eqs. (6) include vertices with all external legs off shell. To circumvent these two problems we have applied a solution procedure based on the use of dispersion relations and a regularization method as outlined in the following sections.

#### A. Solution procedure

Hereafter we shall denote half-off-shell vertices as  $\Gamma_\alpha(p)$ , dropping the trivial parameters for brevity. As noted in the

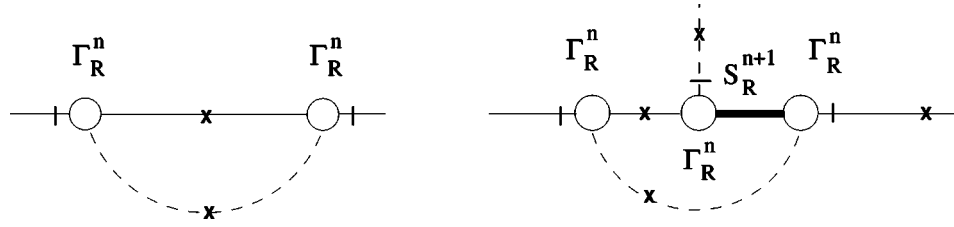


FIG. 2. The pole contribution of iteration  $n+1$  to the self-energy (the left picture) and the vertex (the right picture), as expressed by Eqs. (8)–(12). The notation is as in Fig. 1, with the subscript  $R$  indicating that the vertex and propagator are calculated using only the real parts of the form factors and self-energy functions. The crosses on lines indicate that the corresponding particles are put on their mass shells.

above, Eqs. (6) require the knowledge of the full off-shell vertex. Using the analyticity of the form factors and the self-energy this problem can be bypassed. The imaginary parts of the form factors can be obtained by applying Cutkosky rules to the integrals in Eqs. (6), and we reconstruct the real parts through the application of dispersion relations implemented in an iterative procedure.

As stated in the introduction, we have excluded four- or higher-point vertices from our model. Furthermore, in applying Cutkosky rules we shall only include the channel with the lowest threshold, i.e., the one-pion nucleon channel. This results in the contributions depicted in Fig. 2.

The solution procedure can now be explained best by going in some detail through one complete step of the iterative procedure. From the  $n$ th iteration we have obtained the form factors  $G_{1,2}^n(p^2)$  which define the vertex through Eq. (3) and the self-energy functions  $A^n(p^2)$  and  $B^n(p^2)$  which define the dressed propagator,

$$(\Sigma^n(p))^{-1} = Z_2(\not{p} - m_B) - [A^n(p^2)\not{p} + B^n(p^2)m], \quad (7)$$

where the term in square brackets is the loop contribution  $\Sigma_L^n(p)$  to the self-energy. The parameters  $Z_2$  and  $m_B = m - \delta m$  are renormalization constants as defined in Sec. III B.

The imaginary parts of the form factors and the self-energy functions arise from the pinching-pole term in the loop integrals which can be evaluated using Cutkosky rules [17]. This contribution is labeled by the subscript  $I$ . For the self-energy one has

$$\Sigma_I^{n+1}(p) = -\bar{\Gamma}_{\alpha,R}^n(p) I_{\text{pole}}(p) \Gamma_{\alpha,R}^n(p), \quad (8)$$

where the subscript  $R$  denotes the vertex calculated using only the real parts of the form factors  $G_{1,2}^n$ . The Dirac conjugated vertex is denoted as  $\bar{\Gamma}$ . The remaining integral can be written as

$$I_{\text{pole}}(p) = \frac{1}{8\pi^2} \int d^4k (\not{p} + \not{k} + m) \delta((p+k)^2 - m^2) \times \theta(p_0 + k_0) \delta(k^2 - \mu^2) \theta(-k_0). \quad (9)$$

The explicit form for  $I_{\text{pole}}(p)$  is given in Appendix A. The imaginary parts of  $A^{n+1}(p^2)$ ,  $B^{n+1}(p^2)$  can now readily be written using Eq. (7).

The real parts of the self-energy functions are calculated via the dispersion relations [16],

$$\text{Re } A^{n+1}(p^2) = \frac{\mathcal{P}}{\pi} \int_{w_{th}^2}^{\infty} dp'^2 \frac{\text{Im } A^{n+1}(p'^2)}{p'^2 - p^2}, \quad (10)$$

and similar for  $\text{Re } B(p^2)$ . Here  $w_{th} \equiv (m + \mu)$  is the one-pion threshold, and  $\mathcal{P}$  denotes the principal value integral.

The pole term in the loop integral for the vertex reads

$$\Gamma_{\alpha,I}^{n+1}(p) = J_{\text{pole}}(p) \Gamma_{\alpha,R}^n(p) \quad (11)$$

with

$$J_{\text{pole}}(p) = -\frac{(-1)}{8\pi^2} \int d^4k \Gamma_R^n(p' + k) S_R^{n+1}(p' + k) \bar{\Gamma}_R^n(p' + k) \times (\not{p} + \not{k} + m) \times \delta((p+k)^2 - m^2) \theta(p_0 + k_0) \times \delta(k^2 - \mu^2) \theta(-k_0), \quad (12)$$

where the integral Eq. (12) is independent of  $p'$ , the momentum of the outgoing on-shell nucleon, as shown in Appendix B. The factor  $(-1)$  in Eq. (12) comes from commuting the isospin matrices. The propagator  $S_R^{n+1}$  in Eq. (12) contains only the real parts of  $A^{n+1}$  and  $B^{n+1}$  which have been calculated by virtue of Eqs. (8),(9),(10). Casting  $\Gamma_{\alpha,I}^{n+1}(p)$  in the form of Eq. (3), the imaginary parts of the form factors  $G_{1,2}^{n+1}(p^2)$  are found.

To construct the real parts of the form factors we take advantage of their analytical properties [11],

$$\text{Re } G_i^{n+1}(p^2) = G_i^0(p^2) + \frac{\mathcal{P}}{\pi} \int_{w_{th}^2}^{\infty} dp'^2 \frac{\text{Im } G_i^{n+1}(p'^2)}{p'^2 - p^2}. \quad (13)$$

The first term on the right-hand side of Eq. (13) derives from the equivalent term in Eqs. (6). We use unsubtracted dispersion relations since convergence of the integrals can be guaranteed by the cutoff function introduced in Eq. (18).

There are a few points that need special stressing here.

(i) In calculating the imaginary parts for the  $(n+1)$ st iteration, we retain only the real parts of the form factors and self-energy functions from the  $n$ th iteration, to be consistent with the use in a  $K$ -matrix formalism as explained in Sec. III C.

(ii) Except the depicted cuts, any other kinematically allowed cuts of the loop diagrams [cutting through the blobs in Fig. 2] would correspond to either picking up contributions of higher thresholds or considering four-point vertices, both of which would be inconsistent with the adopted solution scheme.

(iii) In cutting the self-energy loop diagram, dressed vertices at both sides of the cut propagator are taken into account. Seemingly, this is in conflict with the Schwinger-Dyson equation [see Eqs. (6) and Fig. 1], where the second blob would lead to double counting. However, the presence of the two blobs in the *cut* diagram is necessary to sum up *all* contributions from one-pion-nucleon cuts.

(iv) The present method of solution allows one to avoid dealing with the full off-shell vertices present in Eqs. (6). Indeed, as can be seen from Fig. 2, we need only half-off-shell vertices throughout the iteration process.

(v) To calculate the pole contributions of the loop integrals we have applied Cutkosky rules, i.e., put the nucleon and pion lines in the loop integrals on their respective mass shells, as shown in Fig. 2. In the cut propagators, therefore, only physical masses appear. In particular, this implies that the dressing of the pion propagator does not have to be considered in the present approach.

We take  $\Gamma_\alpha^0(m, p, \mu)$  as the zeroth iteration for the vertex [its precise form is specified in Eq. (18)]. At each iteration step, we utilize the dispersion relations Eqs. (13), (10), where  $\text{Im} G_{1,2}(p^2)$ ,  $\text{Im} A(p^2)$ , and  $\text{Im} B(p^2)$  are calculated using Cutkosky rules. In this connection, the following remarks are in order.

*Analyticity.* In principle, the use of the dispersion relations should guarantee that the form factors and the self-energy functions  $A$  and  $B$  be analytic in the complex plane cut from  $w_{\text{th}}^2$  to  $\infty$  along the real axis. However, the actual imaginary parts calculated in the model contain also “unphysical” singularities of the function  $G^0(p^2)$ , see Eq. (18), regularizing the dispersion integrals. This, strictly speaking, invalidates the derivation of the dispersion relations. This problem will be encountered for any nonconstant function  $G^0(p^2)$  unless its singularities are located along the cut.

*Unitarity.* In applying Cutkosky rules, an important qualification is that we neglect the contributions to the imaginary parts that come from the intermediate states including one nucleon and more than one pion. In order that unitarity should hold exactly, the imaginary parts must contain the contributions from all multipion thresholds. In the context of the present work, a rigorous account of, e.g., the two-pion threshold would require computing the imaginary parts of two-loop self-energy and vertex diagrams. Analyses of massive two-loop Feynman diagrams have appeared in the literature recently, including the dispersion relation approach (see, e.g., [29] and references therein). However, such calculations are rather complicated, and we found their application in the present model not feasible.

One may argue that the real function  $G^0$ , which is used presently, could be expressed in terms of a dispersion integral over a function, say  $F^0$ , which would correspond to the discontinuities of the form factors due to all channels opening at higher thresholds not considered explicitly. If this were the case, the presently adopted procedure would be equivalent to adding an extra contribution  $F^0$  to the imaginary parts derived from the loop diagrams. This could possibly account for the two problems just mentioned, but we did not pursue this direction.

## B. Renormalization and regularization

The renormalized nucleon self-energy in Eqs. (6) or Eq. (7) can be written as

$$\Sigma(p) = \Sigma_L(p) - (Z_2 - 1)(\not{p} - m) - Z_2 \delta m. \quad (14)$$

The first term in Eq. (14) is the contribution of pion loops while the last two terms come from the counterterms in the Lagrangian as part of the renormalization procedure.

The construction of the counterterms is based on the usual renormalization procedure [30] as explained by the following example. The Lagrangian, written in terms of the “bare” fields, masses and coupling constant, is

$$\begin{aligned} \mathcal{L} = & \frac{1}{2} (\partial_\nu \phi_B \partial^\nu \phi_B - \mu_B^2 \phi_B^2) + \bar{\psi}_B (i \not{\partial} - m_B) \psi_B \\ & - \frac{g_B}{2m_B} \bar{\psi}_B \gamma^5 (\not{\partial} \phi_B) \psi_B. \end{aligned} \quad (15)$$

Defining the renormalized nucleon field  $\psi = Z_2^{-1/2} \psi_B$ , the renormalized nucleon mass  $m = m_B + \delta m$  and the constant  $f/(2m) = g_B Z_2/(2m_B)$ , Equation (15) can be reformulated as

$$\begin{aligned} \mathcal{L} = & \frac{1}{2} (\partial_\nu \phi \partial^\nu \phi - \mu^2 \phi^2) + \bar{\psi} (i \not{\partial} - m) \psi \\ & - \left( \frac{f}{2m} \bar{\psi} \gamma^5 (\not{\partial} \phi) \psi - Z_2 \delta m \bar{\psi} \psi - (Z_2 - 1) \bar{\psi} (i \not{\partial} - m) \psi \right). \end{aligned} \quad (16)$$

Because we encounter only cut pion lines during the iteration procedure (see Fig. 2), we need only the pole contribution of the pion propagator. Since the pole properties of the renormalized dressed propagator coincide with those of the free one, the pion field and mass need not be renormalized in our approach,  $\phi = \phi_B$ ,  $\mu^2 = \mu_B^2$ . From Eqs. (7) and (14) it can be seen that the renormalization constants  $Z_2$  and  $\delta m$  can also be interpreted as real constants which can always be added when the real part of a function is determined from the imaginary part via a dispersion relation Eq. (10).

The coupling strength  $f$  and the renormalization constants  $Z_2, \delta m$  are determined by fixing  $\Gamma_\alpha(m, m, \mu)$  and the pole structure of the propagator  $S(p)$ ,

$$S^{-1}(m) = 0,$$

$$\text{Res}[S(p), \not{p} = m] = 1, \quad (17)$$

$$\bar{u}(p') \Gamma_\alpha(m, m, \mu) u(p) = \bar{u}(p') \tau_\alpha \gamma^5 g u(p),$$

where the last equation can be reduced to  $G_1(m^2) = g$ , the physical pion-nucleon coupling constant (we take  $g = 13.02$  [31]). The left-hand side of this condition is calculated at the kinematically forbidden point, where all the external legs of the vertex are on-shell. However, this is of no harm for the renormalization prescription. We could choose any convenient renormalization point as long as the form factors calculated at that point are real (see, e.g., [30], where the freedom of the choice of a renormalization procedure is discussed in general).

In the context of the iterative procedure described in the previous section, the constants  $Z_2$  and  $\delta m$  are chosen to provide the correct pole properties of the *converged* propa-

gator. This implies that the pole location and residue of the propagator are off in the course of the first few iterations. To check that this feature is immaterial for the final result, we applied also another solution procedure. Its main difference from the one outlined above is that the renormalization of the propagator is done at each iteration step, insuring the correct pole properties at any iteration. We found that both methods lead to identical results for the converged vertex and propagator. The reason for this is that when convergence has been reached, a nonperturbative solution of Eqs. (6) (under the provisions which have been discussed) has been obtained. The intermediate steps in the iteration procedure at this point are an uninteresting technical detail.

The loop integrals, or rather the dispersion integrals Eqs. (13),(10), will diverge unless a regularization is applied. As part of the regularization procedure, we introduced a form factor  $G^0(p^2)$  (also called the cutoff function) for the bare  $\pi NN$  vertex,

$$\Gamma_\alpha^0(m, p, \mu) = \tau_\alpha \gamma^5 \frac{\not{p} + m}{2m} G^0(p^2), \quad (18)$$

in terms of Eq. (4). The function  $G^0(p^2) \equiv G_{pV}^0(p^2)$  is normalized to  $f$  at  $p^2 = m^2$  and must fall off sufficiently fast at infinity to provide convergence of the integrals. In the numerical example discussed later we used two different functions  $G^0(p^2)$ , see Eqs. (23),(24).

The cutoff function is a phenomenological input of the model. A self-consistent procedure to construct meson-nucleon form factors was presented in Ref. [32], where both nucleons in the vertex are on-shell and the meson is off-shell. There, no phenomenological form factor was needed. We were not successful in implementing a similar approach for half-off-shell form factors in the pion-nucleon vertex, non-trivial solutions of the relevant equations for the self-energy and the  $\pi NN$  vertex did not seem to exist.

### C. Consistency with a $K$ -matrix approach

One motivation for the present model is the construction of form factors and self-energies which can be applied in a  $K$ -matrix approach to  $\pi N$  scattering [21,22]. We outline the  $K$ -matrix method (details can be found in [21]) and in particular address the double-counting issue: by considering only the real part of the form factors and the self-energy functions on the right-hand side of Eqs. (8),(11),(12), we avoid double counting when the calculated vertex and propagator are used in the  $K$ -matrix approach. It should be emphasized that only the one-pion threshold discontinuities are taken into account in both the  $K$ -matrix approach in question and the present model.

The Bethe-Salpeter equation for the  $\pi N$  scattering amplitude  $\mathcal{T}$  can be written in the operator form

$$\mathcal{T} = V + V \mathcal{G} \mathcal{T}. \quad (19)$$

Here,  $V$  is the sum of all irreducible diagrams describing the scattering, and  $\mathcal{G}$  is the free  $\pi N$  propagator.  $\mathcal{G}$  can be decomposed as the sum of the on-shell contribution  $i\delta$  which is imaginary (according to Cutkosky rules), and the off-shell part  $\mathcal{G}^P$  which is real,

$$\mathcal{G} = \mathcal{G}^P + i\delta, \quad (20)$$

where  $\delta$  implies that the corresponding intermediate nucleon and pion are taken on their respective mass shells. The  $K$  operator is introduced by the equation

$$K = V + V \mathcal{G}^P K. \quad (21)$$

Combining the last three equations yields the  $\mathcal{T}$  matrix expressed in terms of the  $K$  matrix,

$$\mathcal{T} = K + K i \delta \mathcal{T}. \quad (22)$$

This is the central equation used in a  $K$ -matrix approach and can schematically be written as  $\mathcal{T} = K/(1 - iK)$ . If  $K$  is Hermitian, the scattering operator  $S = 1 + 2i\mathcal{T}$  will be unitary.

We consider a simplified version of the  $K$ -matrix approach containing only nucleons and pions, with the kernel  $V$  chosen as the sum of the  $s$ - and  $u$ -channel tree diagrams. One way to construct the  $K$  operator is to set  $K = V$  [22], thereby assuming  $\mathcal{G}^P = 0$ , see Eq. (21). Then, by Eq. (22), the  $\mathcal{T}$  matrix will contain the loop diagrams in which only the cut nucleon and pion propagators will enter. Only by using dressed vertices and propagators may one take the  $K$  matrix equal to the sum of skeleton diagrams solely. As implied by Eq. (21), the form factors in these dressed vertices take into account real contributions due to the principal value  $\mathcal{G}^P$ . These are the real parts of the form factors discussed in the previous sections. If we kept both the real and imaginary parts of the form factors and the self-energy functions in Eqs. (8),(11),(12), it would be inconsistent with the  $K$ -matrix approach. In particular, the on-shell contributions  $i\delta$  would be taken into account twice for every  $\pi N$  propagator  $\mathcal{G}$ . An exception are some one-particle irreducible diagrams contributing to the  $\mathcal{T}$  matrix.

It is known that the nucleon and pion degrees of freedom are not enough for a realistic description of  $\pi N$  scattering (for example, the role of both the  $\Delta$  resonance and the  $\rho$  meson is indispensable) [6–9,21,22]. Since in our model we confine ourselves to the pion and the nucleon, no calculations for the  $\pi N$  scattering observables will be presented in this paper.

## IV. NUMERICAL RESULTS

Two sets of calculations were done, corresponding to the two following cutoff function  $G^0(p^2)$ , Eq. (18):

$$G_I^0(p^2) = f \left[ \frac{(\lambda^2 - m^2)^2}{(\lambda^2 - m^2)^2 + (p^2 - m^2)^2} \right]^2 \quad (23)$$

and

$$G_{II}^0(p^2) = f e^{-(p^2 - m^2)^2 / 2dm^4}. \quad (24)$$

The functional dependence of  $G_I^0(p^2)$  is taken from Ref. [6], where it was used as an off-shell form factor in the  $\pi NN$  vertex. We define a parameter  $\Lambda^2 = p_{0.5}^2 - m^2$ , where  $p_{0.5}^2$  is the point at which  $G^0(p^2)$  reduces by a factor of 2 comparing to its maximum value  $f$  (here  $p_{0.5}^2 > m^2$ ). Then, for the calculations with the functions Eq. (23) and Eq. (24),  $\Lambda^2$  equals

TABLE I. Values of the renormalization constants  $f$ ,  $Z_2$ , and  $\delta m$  for the two choices for the function  $G^0(p^2)$ , Eq. (23) and Eq. (24).

Case	$f$	$Z_2$	$\delta m$ (MeV)
(I)	12.42	0.848	-57.4
(II)	12.43	0.848	-55.5

$$\Lambda_I^2(\lambda) = \sqrt{\frac{(\lambda^2 - m^2)^2}{\sqrt{0.5}} - (\lambda^2 - m^2)^2} \quad (25)$$

and

$$\Lambda_{II}^2(d) = \sqrt{-2dm^4 \ln 0.5}, \quad (26)$$

respectively. We find that the iteration procedure described above converges *only* if  $\lambda \leq \lambda_c \approx 1.7$  GeV for  $G_I^0(p^2)$ , and if  $d \leq d_c \approx 1.65$  for  $G_{II}^0(p^2)$ . The corresponding ‘‘critical’’ values for the half-widths can be inferred from Eqs. (25) and (26):  $\Lambda_I^2(\lambda_c) = 1.28$  GeV<sup>2</sup> and  $\Lambda_{II}^2(d_c) = 1.33$  GeV<sup>2</sup>. Results of calculations are presented below for the following two cases:

Case (I). Calculations with the cutoff function Eq. (23), where  $\lambda = \lambda_c = 1.7$  GeV;

Case (II). Calculations with the cutoff function Eq. (24), where  $d = d_c = 1.65$ .

As stated above, the constants  $f$ ,  $Z_2$ , and  $\delta m$  are chosen to satisfy Eqs. (17). The values of these constants for cases (I) and (II) are given in Table I.

The convergence was considered achieved at iteration  $m$  if all the results of iterations  $m+1, \dots, m+20$  were identical to those of iteration  $m$  up to six significant digits. We could impose a very strong convergence criterion since the computer program uses little CPU time. With this criterion, convergence was reached after about 100 iterations. We mention that, for example, the self-energy after ten iterations differs still quite noticeably from the converged result.

A comparison of results obtained with the two different cutoff functions show how these reflect in the final results. The nonperturbative aspects are stressed by comparing the results of the first iteration (basically a one-loop calculation) with those of the converged calculation.

#### A. Results for the half-off-shell form factors

The imaginary parts of the form factors  $G_{PV}(p^2)$  and  $G_{PS}(p^2)$  are shown in Fig. 3. The results of calculations for the two cutoff functions introduced in Eqs. (23) and (24) are shown next to each other. For case (II) the tails of the form factors at large off-shellness are suppressed due to the exponential in the cutoff function. Independent of the choice of the cutoff function there is a marked difference in the results of the first iteration (dotted curve) and the converged results for the pseudovector form factor. The reason for this difference is the (small) pseudoscalar component of the final form factor. The converged and first iteration results for the pseudoscalar form factor differ much less, as can be seen from the bottom panels of Fig. 3.

The real parts of the form factors are shown in Fig. 4. The top panels show the pseudovector form factor  $G_{PV}(p^2)$  (the

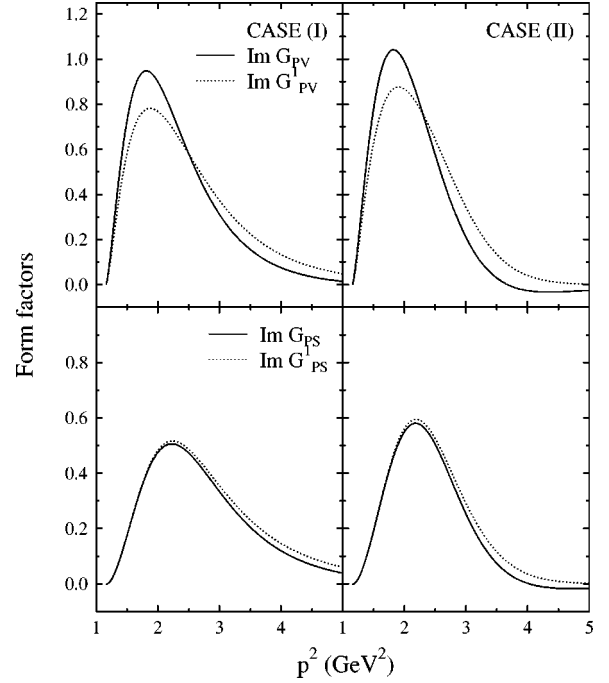


FIG. 3. The imaginary parts of the pseudovector and pseudoscalar  $\pi NN$  form factors as functions of the momentum squared of the off-shell nucleon, defined in Eq. (4). The calculations correspond to the two cutoff functions, Eq. (23) (the left panels) and Eq. (24) (the right panels). The solid (respective dotted) curves show the converged (respective first iteration) results.

solid line) together with the zeroth iteration form factor  $G_{PV}^0(p^2)$  (the dotted line) which equals the cutoff functions Eq. (23) (left) and Eq. (24) (right). It is seen that the bulk of  $G_{PV}(p^2)$  is contained already in  $G_{PV}^0(p^2)$ , and only a small part comes from the loop corrections. This manifests itself also in the small difference between the constant  $f$  and the physical coupling constant  $g$ , as can be read from Table I. We conclude that, in the present model, the shape of the converged form factor  $G_{PV}$  depends strongly on the phenomenologically introduced cutoff function. The middle panels of Fig. 4 give more insight in the role of the pion dressing. There, the real part of the pseudoscalar form factor  $G_{PS}(p^2)$  of the first iteration (the dashed line) is shown together with the converged result (the solid line). Since the zeroth iteration vertex is chosen purely as a pseudovector [Eq. (18)],  $G_{PS}(p^2)$  appears solely due to the dressing. Also shown is the difference  $\text{Re}[G_{PV}(p^2) - G_{PV}^0(p^2)]$  which is the dressing contribution to the real part of the pseudovector form factor (the dash-dotted and dotted lines for the first iteration and the converged result, respectively). Note that the deviation of the nonperturbative result from that of the first iteration is considerable for this quantity. The ratio of the real parts of the  $G_{PS}(p^2)$ - and  $G_{PV}(p^2)$ -form factors is given in the bottom panel of Fig. 4. It is small below the pion threshold [e.g.,  $G_{PS}(w_{th}^2)/g$  is about 2.1% for both cases (I) and (II)], but becomes larger at higher  $p^2$ . Note that  $G_{PV}(p^2)$  decreases for case (II) faster than for case (I), whereas the behavior of  $G_{PS}(p^2)$  for the two cases is comparable. This explains why the absolute value of  $(\text{Re}G_{PS}(p^2))/(\text{Re}G_{PV}(p^2))$  grows faster for case (II) than for case (I).

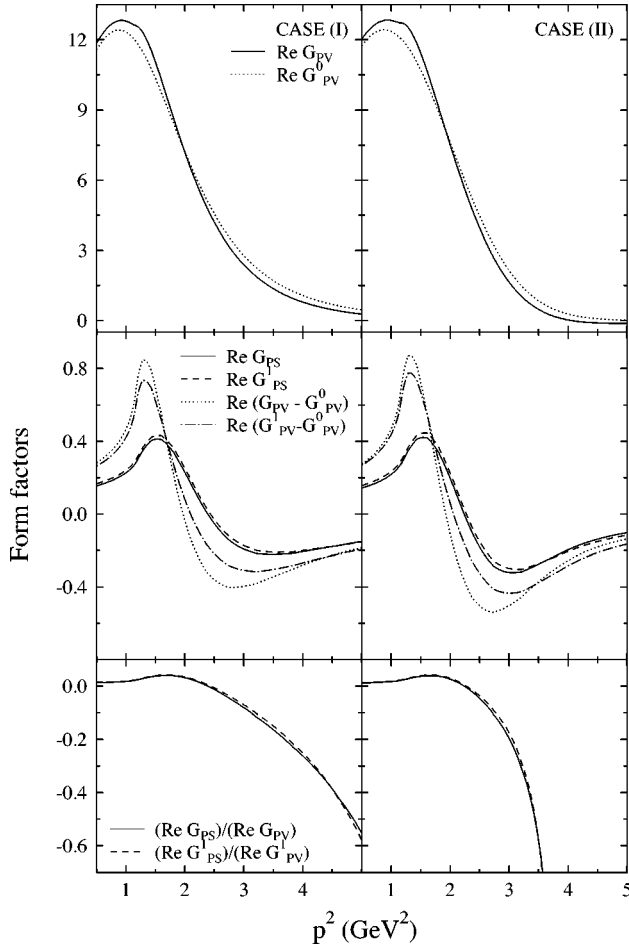


FIG. 4. The real parts of the pseudovector and pseudoscalar  $\pi NN$  form factors as functions of the momentum squared of the off-shell nucleon, defined in Eq. (4). The calculations correspond to the two cutoff functions Eq. (23) (the left panels) and Eq. (24) (the right panels). In the top panels the zeroth iteration and the converged form factors are given by the dotted and solid lines, respectively. In the middle panels the converged results and those of the first iteration are shown for the pseudoscalar form factor and the loop contribution to the pseudovector form factor. The bottom panels show the ratio of the pseudoscalar and pseudovector form factors, where the solid (respectively dashed) curves correspond to the converged (respectively first iteration) results.

We remark that admixtures of the pseudovector and pseudoscalar pion-nucleon couplings have been studied in the past in connection with the  $NN$  and  $\pi N$  scattering processes, where the vertex has been determined by adjusting phenomenological parameters to fit data (see discussions in [5–7,21]). In those calculations the admixture is assumed to be constant. Instead, the present results indicate that the ratio is strongly dependent on the momentum of the off-shell nucleon. Evidence for large pseudoscalar admixtures for far off-shell momenta has also been observed in calculations of pion photoproduction [33].

### B. Results for the self-energy

The imaginary and real parts of the functions  $A(P^2)$  and  $B(P^2)$  are shown in Figs. 5 and 6, respectively. The solid (dotted) lines are the converged (first iteration) results. One can see that these functions approach zero faster for case (II)

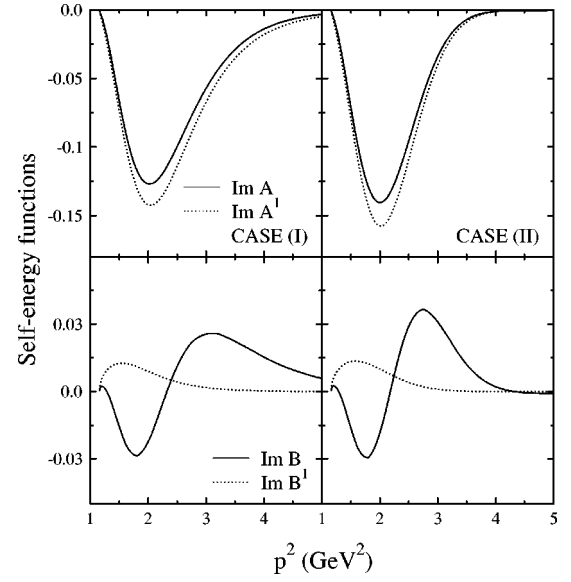


FIG. 5. The imaginary parts of the self-energy functions  $A(p^2)$  and  $B(p^2)$ , as defined in Eq. (7). The calculations correspond to the two cutoff functions Eq. (23) (the left panels) and Eq. (24) (the right panels). The solid (respectively dotted) curves are the converged (respectively first iteration) results.

than for case (I). Of course, this is entailed by the softer behavior of  $G_{pv}^0(p^2)$  for case (II) as opposed to case (I) (see Fig. 4). The difference between the converged results and those of the first iteration is substantial, especially for the function  $B(p^2)$ . The on-shell value  $\Sigma_L(m) = m[A(m^2) + B(m^2)] = Z_2 \delta m$  is negative and equals  $-48.8$  MeV for case (I) and  $-47.2$  MeV for case (II), see Table I. Please note that if we had chosen smaller values for the cutoff, these self-energy corrections would have been less. For comparison, we mention that the contribution to the nucleon mass shift from one-pion loop calculated in baryon chiral perturbation theory yields a nucleon mass shift of about  $-15$  MeV [34].

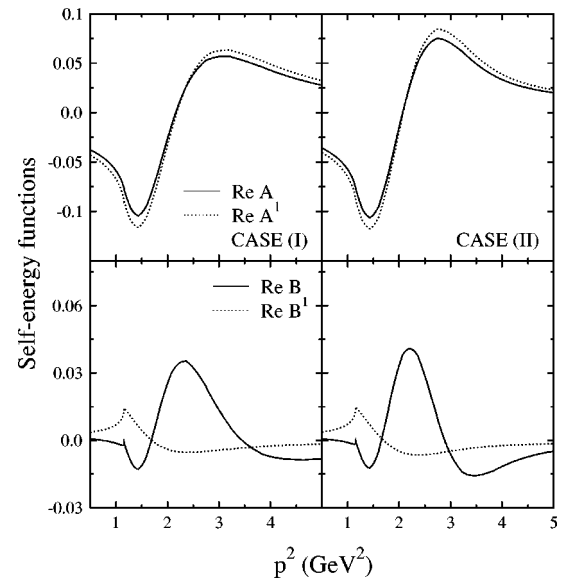


FIG. 6. The same as in Fig. 5, but for the real parts of  $A(p^2)$  and  $B(p^2)$ .

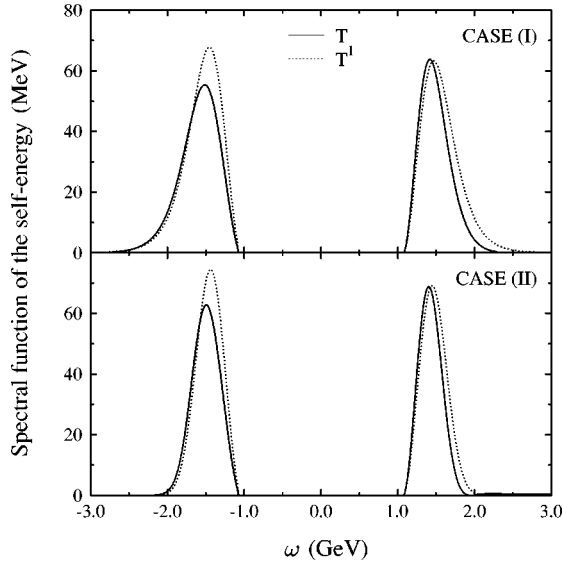


FIG. 7. The self-energy spectral function  $T(\omega)$  as function of invariant mass of the nucleon. The upper (respective lower) panel corresponds to the calculations with the cutoff function Eq. (23) [respective Eq. (24)]. The solid (respective dashed) curves are the converged (respective first iteration) results.

Having obtained  $A(p^2)$  and  $B(p^2)$ , one can find the spectral function of the self-energy  $T(\omega)$  from Eq. (A9). Figure 7 shows the spectral function for the two cases (the upper and lower panels). The dotted and solid lines are, respectively, the first iteration and the converged spectral function found in our model. In spite of the fact that  $\text{Im } B^1(p^2)$  differs considerably from  $\text{Im } B(p^2)$ , having the opposite sign at some momenta squared (see Fig. 5), the spectral function remains positive for all iterations (as it should).

The spectral function of the nucleon propagator was recently considered in Ref. [20] whose approach is, however, different from the present work. In particular, there the vertex was not calculated consistently with the nucleon propagator.

## V. CONCLUSIONS

We have presented a solution procedure for the Schwinger-Dyson equation to obtain consistently the nucleon self-energy and the half-off-shell pion-nucleon vertex. Retaining the nonperturbative aspects of the equations is important. We observe a large difference between the simple one-loop results and those of the converged procedure. As part of the regularization procedure, we have introduced a cutoff function. We found that in our model there exists a critical half-width, of the order of  $1.3 \text{ GeV}^2$ , below which a nonperturbative solution can be obtained. Particularly noteworthy is that even though the dressed vertex near threshold is largely pseudovector in nature, we find sizable admixtures of pseudoscalar coupling at large off-shell nucleon momenta.

It is important to realize that off-shell form factors and self-energies cannot be directly measured. The observables in quantum field theory are obtained from the  $S$  matrix, not the Green's functions. The latter will depend on the representation of the fields in the Lagrangian of the theory, whereas the former do not. In principle, observables should not depend on the regularization and renormalization proce-

dures chosen. This, however, does not apply to the Green's functions. To draw quantitative conclusions about physical processes, one should treat all off-shell ingredients of a model consistently, calculating them with the same Lagrangian and adhering to the same model assumptions. For example, the present model for the pion-nucleon off-shell form factors and the nucleon self-energy can be consistently utilized in a  $K$ -matrix approach to  $\pi N$  scattering, as shown in Sec. III C.

Although the present work deals with  $\pi NN$  vertices where one of the nucleons is off-shell, we mention here that there exists a large amount of work on the form factor  $G_1(m^2, m^2, q^2)$  [see Eq. (1)] for on-shell nucleons and an off-shell pion (see, e.g., [32,35,36] and references therein). In particular, in Ref. [32] a system of  $N$ ,  $\pi$ ,  $\Delta$ ,  $\rho$ ,  $\epsilon$ , and  $\omega$  hadrons is considered in a consistent field-theoretical framework. The approach of Ref. [35] is based on a meson-exchange model for  $\pi N$  scattering, where, apart from the nucleon and the pion, also  $\Delta$  isobar and correlated  $\pi\pi$  exchange contributions are included. As mentioned before, the  $\Delta$  resonance and the  $\rho$  meson are important ingredients in a quantitative description of  $\pi N$  scattering and pion photoproduction. Therefore, one should expect these degrees of freedom to play a prominent role in a realistic model for pion-nucleon form factors. In the present work, only nucleon and pion fields are included, and only discontinuities associated with the one-pion threshold are taken into account. In this simplified model we focus on nonperturbative aspects of the consistent dressing of the pion-nucleon vertex and the nucleon self-energy. Contributions to the imaginary parts from higher thresholds can be included in our model either explicitly, by allowing intermediate states with two or more pions, or effectively, by considering baryon and meson resonances (for example,  $\Delta$  and  $\rho$ ). This extension of the model is in progress.

## ACKNOWLEDGMENTS

This work was part of the research program of the ‘‘Stichting voor Fundamenteel Onderzoek der Materie’’ (FOM) with financial support from the ‘‘Nederlandse Organisatie voor Wetenschappelijk Onderzoek’’ (NWO). We would like to thank Alex Korchin and Rob Timmermans for discussions.

## APPENDIX A: THE SELF-ENERGY

Here some details on the evaluation of the imaginary part of the nucleon self-energy are given. To calculate the imaginary parts of the self-energy functions, we need to evaluate the pole contribution  $I_{\text{pole}}(p)$  as given in Eq. (9). In general the integral can be expressed as  $I_{\text{pole}}(p) = \gamma_\mu \tilde{I}_1^\mu(p) + \tilde{I}_2(p)$ , where  $\tilde{I}_1^\mu$  and  $\tilde{I}_2$  are scalars in spinor space. Since the only Lorentz vector in the problem is  $p^\mu$ ,  $\tilde{I}_1^\mu$  must be proportional to it,  $\tilde{I}_1^\mu(p) = [(\tilde{I}_1 \cdot p)/p^2] p^\mu$ . Hence, one may write  $I_{\text{pole}}(p) = \not{p} I_1(p^2) + I_2(p^2)$ , where  $I_1(p^2) = (\tilde{I}_1 \cdot p)/p^2$  and  $I_2(p^2) = \tilde{I}_2(p^2)$  are Lorentz scalars. They equal



$$I_1(p^2) = \frac{p^2 + m^2 - \mu^2}{32\pi p^4} r(p^2) \theta(p^2 - (m + \mu)^2), \quad (\text{A1})$$

$$I_2(p^2) = \frac{m}{16\pi p^2} r(p^2) \theta(p^2 - (m + \mu)^2). \quad (\text{A2})$$

where  $r(p^2) = \sqrt{\lambda(p^2, m^2, \mu^2)}$ , with the Källén function defined as  $\lambda(x, y, z) \equiv (x - y - z)^2 - 4yz$ . Using these expressions and introducing the shorthand notation,  $g_{1,2} \equiv \text{Re } G_{1,2}^n(p^2)$ , the imaginary parts of the self-energy functions can be determined from Eqs. (7),(8),(3),

$$\begin{aligned} \text{Im } A^{n+1}(p^2) &= 3 \left( -(g_1 - g_2)^2 I_1(p^2) + 2(g_1 - g_2) g_2 \frac{I_2(p^2)}{m} - g_2^2 \frac{p^2 I_1(p^2)}{m^2} \right) \\ &= -\frac{3}{32\pi p^2} r(p^2) \theta(p^2 - (m + \mu)^2) \left\{ \frac{p^2 + m^2 - \mu^2}{p^2} g_1^2 + \left( \frac{5p^2 + m^2 - \mu^2}{p^2} + \frac{p^2 + m^2 - \mu^2}{m^2} \right) g_2^2 \right. \\ &\quad \left. - 2 \frac{3p^2 + m^2 - \mu^2}{p^2} g_1 g_2 \right\}, \end{aligned} \quad (\text{A3})$$

$$\begin{aligned} \text{Im } B^{n+1}(p^2) &= 3 \left( (g_1 - g_2)^2 \frac{I_2(p^2)}{m} - 2(g_1 - g_2) g_2 \frac{p^2 I_1(p^2)}{m^2} + g_2^2 \frac{p^2 I_2(p^2)}{m^3} \right) = \frac{3}{16\pi p^2} r(p^2) \theta(p^2 - (m + \mu)^2) \\ &\quad \times \left\{ g_1^2 + \frac{2p^2 + 2m^2 - \mu^2}{m^2} g_2^2 - \frac{p^2 + 3m^2 - \mu^2}{m^2} g_1 g_2 \right\}, \end{aligned} \quad (\text{A4})$$

the factor 3 in the above equations results from the multiplication of the isospin matrices,  $\tau_\alpha \tau_\alpha = 3$ , and the minus sign in front of  $I_1(p^2)$  from commuting the  $\gamma^5$  matrices. The real parts of  $A^{n+1}(p^2)$  and  $B^{n+1}(p^2)$  are found by applying dispersion relations Eq. (10), where all integrals are done numerically.

For later use, the dressed nucleon propagator is written as

$$\begin{aligned} (S(p))^{-1} &= Z_2(\not{p} - m_B) - [\text{Re } A(p^2)\not{p} + \text{Re } B(p^2)m] \\ &= \alpha(p^2)[\not{p} - \xi(p^2)], \end{aligned} \quad (\text{A5})$$

where

$$\begin{aligned} \alpha(p^2) &= Z_2 - \text{Re } A(p^2), \\ \xi(p^2) &= \frac{Z_2(m - \delta m) + \text{Re } B(p^2)m}{\alpha(p^2)}. \end{aligned} \quad (\text{A6})$$

The spectral function of the self-energy is introduced through

$$\Sigma_L(p) = \zeta(\omega) \Lambda^+(\not{p}) + \zeta(-\omega) \Lambda^-(\not{p}), \quad (\text{A7})$$

where  $\Lambda^\pm(\not{p}) = (\pm \not{p} + \omega)/(2\omega)$  are the projectors on positive- and negative-energy states of the nucleon with the invariant mass  $\omega = \sqrt{p^2} > 0$ . The spectral function can now be defined as [16]

$$T(\pm\omega) = \mp \frac{1}{\pi} \text{Im } \zeta(\pm\omega). \quad (\text{A8})$$

Equating the right-hand side of Eq. (A7) and the form of  $\Sigma_L(p)$  from Eq. (7) yields

$$T(\pm\omega) = -\frac{1}{\pi} [\omega \text{Im } A(p^2) \pm m \text{Im } B(p^2)]. \quad (\text{A9})$$

## APPENDIX B: THE FORM FACTORS

The calculation of the imaginary parts of the form factors can be reduced to computing one-dimensional integrals which are done numerically. First consider the integral on the right-hand side of Eq. (12).  $J_{\text{pole}}$  can be split as  $J_{\text{pole}} = \gamma_\mu \tilde{J}_1^\mu + \tilde{J}_2$ , where  $\tilde{J}_1^\mu$  and  $\tilde{J}_2$  are scalars in spinor space, and a possible rank-2 tensor structure vanishes since  $\bar{u}(p') \not{p}' = \bar{u}(p') m$ . For the same reason  $\tilde{J}_1^\mu$  is proportional to only the vector  $p^\mu$ . Following the same argumentation as used in Appendix A, we can write

$$J_{\text{pole}} = \not{p} J_1 + J_2, \quad (\text{B1})$$

where we have introduced the Lorentz scalars  $J_1$  and  $J_2$ . To write down expressions for  $J_1$  and  $J_2$ , we define the following functionals:

$$K_1[f] \equiv \int_{-1}^1 dx \frac{f(w'^2)}{\alpha(w'^2)}, \quad (\text{B2})$$

$$K_2[f] \equiv \int_{-1}^1 dx x \frac{f(w'^2)}{\alpha(w'^2)}, \quad (\text{B3})$$

$$K_3[f] \equiv \int_{-1}^1 dx \frac{f(w'^2)}{\alpha(w'^2)[w'^2 - \xi^2(w'^2)]}, \quad (\text{B4})$$

$$K_4[f] \equiv \int_{-1}^1 dxx \frac{f(w'^2)}{\alpha(w'^2)[w'^2 - \xi^2(w'^2)]}, \quad (\text{B5})$$

where  $f$  is any function for which the integrals exist,  $\alpha$  and  $\xi$  are given by Eq. (A6) for the  $(n+1)$ st iteration, and

$$w'^2 = (p' + k)^2 = m^2 + \mu^2 - \frac{p^4 - (m^2 - \mu^2)^2}{2p^2} - \frac{r(p^2)^2}{2p^2} x, \quad (\text{B6})$$

with  $x$  being the cosine of the polar angle between the three vectors  $\vec{p}'$  and  $\vec{k}$ . Now  $J_1$  and  $J_2$  can be written as

$$\begin{aligned} J_1 \equiv J_1(p^2) = & - \left\{ (K_1 - K_2) \left[ \frac{p^2 + m^2 - \mu^2}{2p^2} \right. \right. \\ & \times \left( g_1 g_2 + \frac{\xi - 4m}{2m} g_2^2 \right) + \frac{g_2^2}{2} \left. \right\} + (K_3 - K_4) \\ & \times \left[ \left( \frac{p^2 + m^2 - \mu^2}{p^2} \frac{\xi}{4m} - \frac{m^2 - \mu^2}{2p^2} \right) \right. \\ & \times [m g_1 + (\xi - m) g_2]^2 \left. \right\} \frac{r(p^2)}{16\pi p^2} \theta(p^2 - (m + \mu)^2) \end{aligned} \quad (\text{B7})$$

and

$$\begin{aligned} J_2 \equiv J_2(p^2) = & - \left\{ (K_1 + K_2) \left[ \left( \frac{\xi - 4m}{2m} + \frac{p^2 + m^2 - \mu^2}{4m^2} \right) g_2^2 + g_1 g_2 \right] \right. \\ & + (K_3 + K_4) \left[ \left( \frac{\xi - 2m}{2m} + \frac{p^2 + m^2 - \mu^2}{4m^2} \right) \right. \\ & \times [m g_1 + (\xi - m) g_2]^2 \left. \right\} \frac{r(p^2)}{16\pi p^2} \theta(p^2 - (m + \mu)^2). \end{aligned} \quad (\text{B8})$$

Since for a given  $f$  in Eqs. (B2)–(B5) the  $K_i$  are functions of  $p^2$  only, Eqs. (B7), (B8), (B1) show that  $J_{\text{pole}}$  depends only on the Lorentz vector  $p$  and does not depend on  $p'$  as it might appear from the right-hand side of Eq. (12).

Using Eqs. (B1), (11), (3), one obtains for the imaginary parts of the form factors:

$$\text{Im } G_1^{n+1}(p^2) = g_1 J_2(p^2) + \left( \frac{m^2 - p^2}{m^2} g_2 - g_1 \right) J_1(p^2) \quad (\text{B9})$$

and

$$\text{Im } G_2^{n+1}(p^2) = g_2 J_2(p^2) + (g_2 - g_1) J_1(p^2), \quad (\text{B10})$$

where  $J_1$  and  $J_2$  are given by Eqs. (B7) and (B8). Finally, Eq. (13) is applied to obtain the real parts of the  $(n+1)$ st iteration for the form factors.

- 
- [1] E. M. Nyman, Nucl. Phys. **A160**, 517 (1971).  
[2] S. Kondratyuk, G. Martinus, and O. Scholten, Phys. Lett. B **418**, 20 (1998).  
[3] Yi Li, M. K. Liou, and W. M. Schreiber, Phys. Rev. C **57**, 507 (1998).  
[4] A. Yu. Korshin, O. Scholten, and F. de Jong, Phys. Lett. B **402**, 1 (1997).  
[5] F. L. Gross, J. W. Van Orden, and K. Holinde, Phys. Rev. C **45**, 2094 (1992).  
[6] F. Gross and Y. Surya, Phys. Rev. C **47**, 703 (1993).  
[7] B. C. Pearce and B. K. Jennings, Nucl. Phys. **A528**, 655 (1991).  
[8] C. Schütz, J. W. Durso, K. Holinde, and J. Speth, Phys. Rev. C **49**, 2671 (1994).  
[9] T. Sato and T.-S. H. Lee, Phys. Rev. C **54**, 2660 (1996).  
[10] K. Nakayama, A. Szczurek, C. Hanhart, J. Haidenbauer, and J. Speth, Phys. Rev. C **57**, 1580 (1998); J. Haidenbauer, C. Hanhart, J. Speth, K. Nakayama, and J. W. Durso, in *Book of Abstracts of the 8th International Conference on the Structure of Baryons*, Baryons'98, Bonn, 1998, p. 84.  
[11] A. Bincer, Phys. Rev. **118**, 855 (1960).  
[12] E. M. Nyman, Nucl. Phys. **A154**, 97 (1970); M. G. Hare, Ann. Phys. (N.Y.) **74**, 595 (1972).  
[13] H. W. L. Naus and J. H. Koch, Phys. Rev. C **36**, 2459 (1987); P. C. Tiemeijer and J. A. Tjon, *ibid.* **42**, 599 (1990); J. W. Bos and J. H. Koch, Nucl. Phys. **A563**, 539 (1993); H. C. Dönges, M. Schäfer, and U. Mosel, Phys. Rev. C **51**, 950 (1995).  
[14] M. Ida, Phys. Rev. **136**, B1767 (1964); G. N. Epstein, Phys. Lett. **79B**, 195 (1978).  
[15] W. T. Nutt and C. M. Shakin, Phys. Rev. C **16**, 1107 (1977).  
[16] N. N. Bogoliubov and D. V. Shirkov, *Introduction to The Theory of Quantized Fields* (Interscience, New York, 1959), Chap. IX.  
[17] R. E. Cutkosky, J. Math. Phys. **1**, 429 (1960); G. 't Hooft and M. J. G. Veltman, Diagrammar, CERN Yellow Report 73-09.  
[18] W. D. Brown, R. D. Puff, and L. Wilets, Phys. Rev. C **2**, 331 (1970).  
[19] G. Krein, M. Nielsen, R. D. Puff, and L. Wilets, Phys. Rev. C

- 47, 2485 (1993); M. E. Bracco, A. Eiras, G. Krein, and L. Wilets, *ibid.* **49**, 1299 (1994).
- [20] C. A. da Rocha, G. Krein, and L. Wilets, Nucl. Phys. **A616**, 625 (1997).
- [21] P. F. A. Goudsmit, H. J. Leisi, E. Matsinos, B. L. Birbrair, and A. B. Gridnev, Nucl. Phys. **A575**, 673 (1994).
- [22] O. Scholten, A. Yu. Korchin, V. Pascalutsa, and D. Van Neck, Phys. Lett. B **384**, 13 (1996).
- [23] S. Kamefuchi, L. O’Raifeartaigh, and A. Salam, Nucl. Phys. **28**, 529 (1961).
- [24] S. Scherer and H. W. Fearing, Phys. Rev. C **51**, 359 (1995); H. W. Fearing, Phys. Rev. Lett. **81**, 758 (1998).
- [25] R. M. Davidson and G. I. Poulis, Phys. Rev. D **54**, 2228 (1996).
- [26] J. Adam, Jr., F. Gross, and J. W. Van Orden, nucl-th/9708002.
- [27] E. Kazes, Nuovo Cimento **13**, 1226 (1959).
- [28] V. B. Berestetskii, E. M. Lifshitz, and L. P. Pitaevskii, *Quantum Electrodynamics* (Pergamon, New York, 1982), pp. 474 and 476.
- [29] S. Bauberger and M. Böhm, Nucl. Phys. **B445**, 25 (1995); A. Frink, J. G. Körner, and J. B. Tausk, hep-ph/9709490 P. Post and J. B. Tausk, Mod. Phys. Lett. A **11**, 2115 (1996).
- [30] S. Weinberg, *The Quantum Theory of Fields*, Vol. 1 and 2 (Cambridge University Press, Cambridge, England, 1996).
- [31] A. Yu. Korchin, O. Scholten, and R. G. E. Timmermans, Phys. Lett. B **438**, 1 (1998).
- [32] J. Flender and M. F. Gari, Phys. Rev. C **51**, R1619 (1995).
- [33] D. Drechsel, O. Hanstein, S. S. Kamalov, and L. Tiator, nucl-th/9807001.
- [34] Ulf-G. Meissner, Czech. J. Phys. **45**, 153 (1995).
- [35] C. Schütz, J. Haidenbauer, and K. Holinde, Phys. Rev. C **54**, 1561 (1996).
- [36] S. A. Coon and M. D. Scadron, Phys. Rev. C **23**, 1150 (1981); A. W. Thomas and K. Holinde, Phys. Rev. Lett. **63**, 2025 (1989); T.-S. H. Lee, nucl-th/9502005; K.-F. Liu, S.-J. Dong, and T. Draper, Phys. Rev. Lett. **74**, 2172 (1995); G. Holzwarth and R. Machleidt, Phys. Rev. C **55**, 1088 (1997).